



# EURISOL DS Project

## Deliverable M3

### In-beam tests to validate design choices

*Planned Date (month): 45*

*Achieved Date (month): 45*

*Lead Contractor(s):*

**U-LIVERPOOL**

**GANIL**

**CNRS/IN2P3**

**INFN**

**NIPNE**

**JYU**

**UW**

**SAS**

**STFC**

---

**Project acronym:** *EURISOL DS*

**Project full title:** *EUROPEAN ISOTOPE SEPARATION ON-LINE  
RADIOACTIVE ION BEAM FACILITY*

**Start of the Project:** *1<sup>st</sup> February 2005*

**Duration of the project:** *54 months*



This document presents the following reports on 5 in-beam tests to validate the proposed design concepts and simulation tools for experimental programmes at the EURISOL facility:

In-beam Validation of the Recoil Separator Design Concept for EURISOL

In-beam Validation of the FAZIA Design Concept for EURISOL

Direct Reactions at EURISOL: In-beam tests to validate the design of an array for light charged-particle and gamma-ray measurements

In-beam validation of the Paul trapping of low energy radioactive ions and direct detection of the beta-decay

Development and validation of neutron detection simulations for EURISOL



# In-beam Validation of the Recoil Separator Design

## Concept for EURISOL

### Physics Motivation

The study of the heaviest elements is a very important component of the physics case for EURISOL. Key experiments have been proposed to perform in-beam  $\gamma$ -ray and conversion-electron spectroscopy experiments to elucidate their structure; to probe the properties of low-lying states through optical spectroscopy measurements; and to investigate the synthesis and decay of superheavy elements. The intense neutron-rich beams available at EURISOL will allow the study of heavy nuclei that cannot be produced through reactions with stable beams, allowing the deformed shell gap at  $N=162$  and the possible spherical shell gap at  $N=184$  to be approached, as well as extending the range of spin and excitation energy at which the nuclei are populated.

A common requirement that has been identified for all of these experimental programmes is a highly efficient recoil separator or recoil mass spectrometer with a beam suppression factor of at least  $10^{12}$ . It is anticipated that such a device should also be suitable for a wide range of other experiments involving fusion-evaporation reactions. The detailed designed criteria for such a recoil separator for EURISOL are summarized at the end of this document.

### Outline of Challenges and Conceptual Solution

While many recoil separator devices are in operation at nuclear physics laboratories around the world, none has been specifically designed for dealing with the very high intensities of radioactive beams that are envisaged for EURISOL. In general they have been designed for use with stable beams with the key performance criteria of high transport efficiency and high beam suppression factor. Many separators also have the capability to separate recoiling ions according to the ratio of their mass ( $A$ ) and charge state ( $q$ ), and for these separators the resolution in  $A/q$  is also an important design criterion. What is generally less important is where the unreacted primary beam is deposited, because once stopped the stable beam ions do not cause experimental difficulties.

Clearly this will cease to be the case in experiments with EURISOL that require radioactive beam intensities of up to  $10^{12}$  particles per second. Typical beam species that are proposed for these experiments include  $^{132}\text{Sn}$  and  $^{92}\text{Kr}$ . The decay chains of both of these nuclides involve 4  $\beta$  decays to



reach a stable nuclide, with half-lives ranging from 1.8 s for  $^{92}\text{Kr}$  to 76 h for  $^{132}\text{Te}$ . This leads to the additional design criterion for a recoil separator for heavy element studies with EURISOL that the primary beam should be deposited in a controlled fashion. The location where the beam is stopped can be in a heavily shielded cave to prevent the radioactivity from causing high background levels in the experimental apparatus and to allow user access to the equipment on shorter timescales after the beam is switched off. Another, more elaborate possibility could be to recycle the radioactive beam, although the feasibility of this remains to be investigated.

The conceptual solution proposed to meet the design criteria is illustrated schematically in figure 1. The beam will be transported straight through a Wien filter that will form the first stage of the recoil separator. The beam can then be dealt with as appropriate. The reaction products that are of interest for the physics experiments will be deviated by the Wien filter. The remainder of the recoil separator, which could comprise one or several deflecting elements plus focusing elements, will be used to collect these ions and transport them with the highest possible efficiency to the focal plane detector system, while at the same time maximally suppressing scattered beam particles.

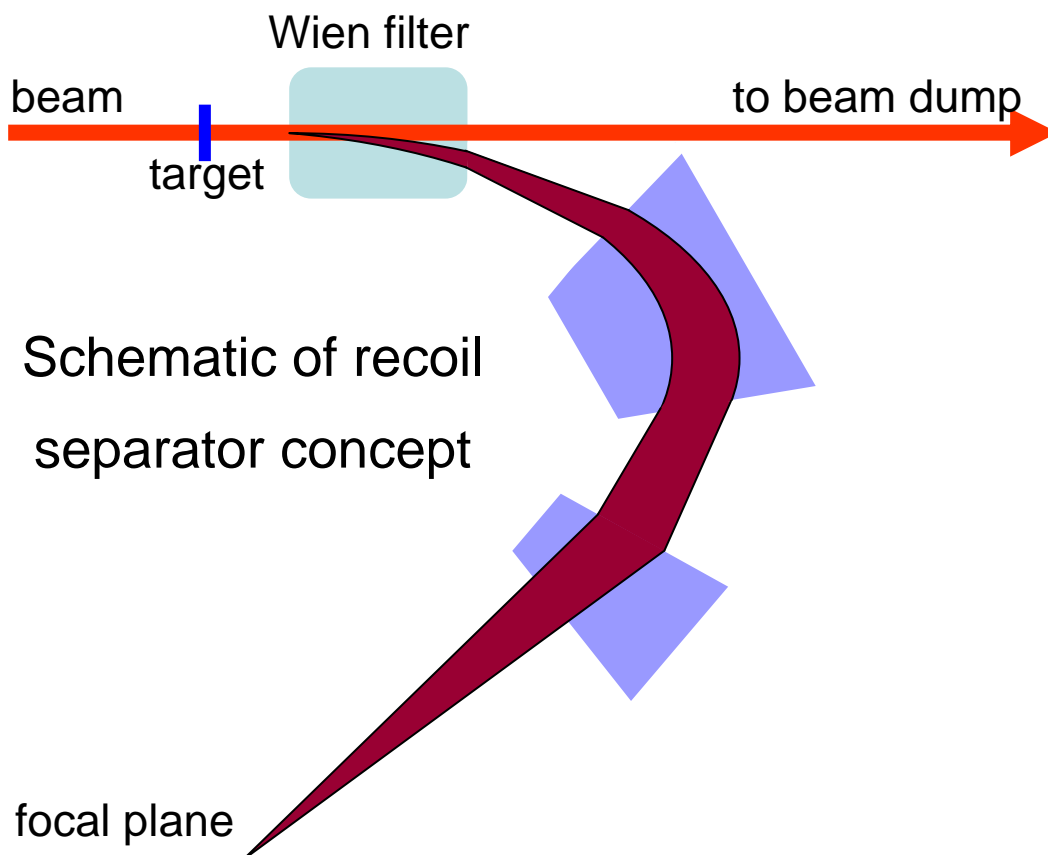


Figure 1: Schematic of the recoil separator design concept.



## Experimental Details of Validation Test

An in-beam test to validate the proposed design concept was performed using VAMOS at the GANIL facility. This test was part of a wider programme to investigate the feasibility of using VAMOS in heavy element studies, which will also be of benefit to studies proposed with SPIRAL2. VAMOS is a versatile recoil separator device that has a Wien filter as its first separation element (see figure 2). This test represented the first attempt using the novel idea of setting the Wien filter to direct the beam straight through, allowing the beam to be dumped in a controlled manner. The evaporation residues were then transported to the focal plane. Beam optics simulations indicated that this mode should not affect the transmission compared with the standard mode of Wien filter operation and that a better degree of beam suppression should be achievable.

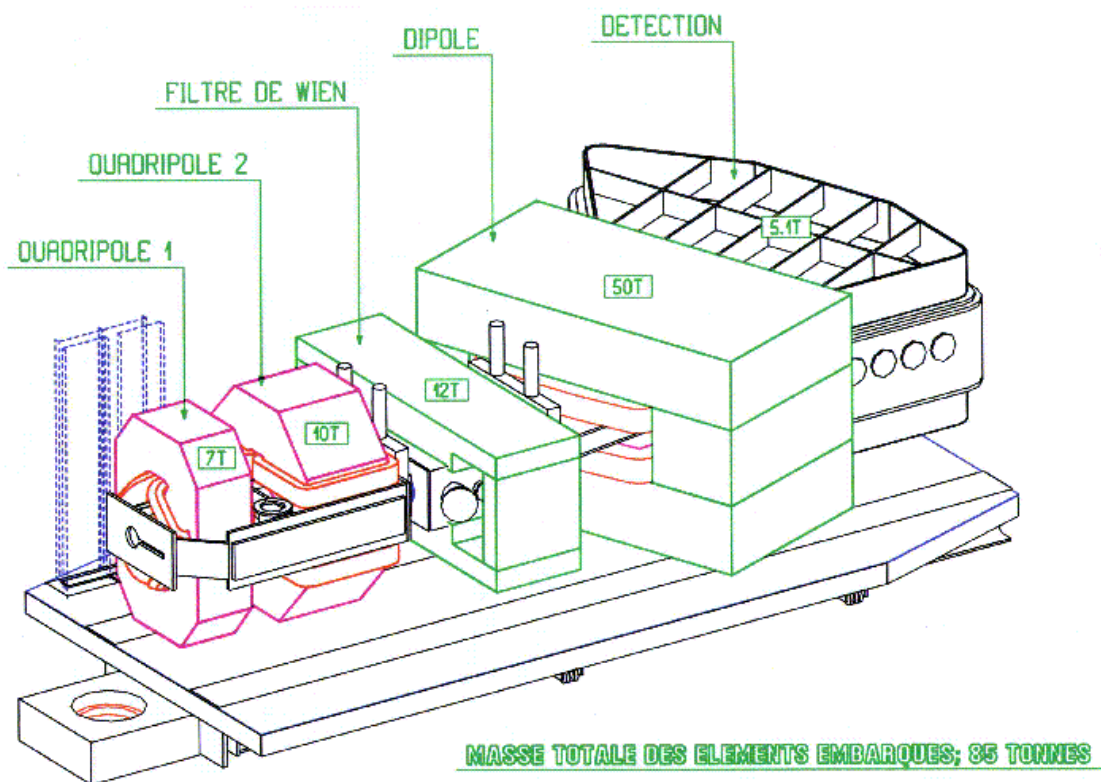


Figure 2: The recoil separator VAMOS used for the in-beam validation.

Three different reactions were used in the tests. The results presented here are from the reaction  $^{22}\text{Ne} + ^{197}\text{Au}$ , which produces the 5n evaporation channel  $^{214}\text{Ac}$  with a maximum cross section of 2.87 mb at a bombarding energy of 114.5 MeV.



## Results

The time of flight was measured between EXOGAM Ge detectors at the target position and the Si detector at the VAMOS focal plane. Figure 3 shows the spectrum of the time of flight versus the recoil energy measured in the Si detector. It is clear from this spectrum that the evaporation residues (recoils) could be distinguished from the scattered beam particles.

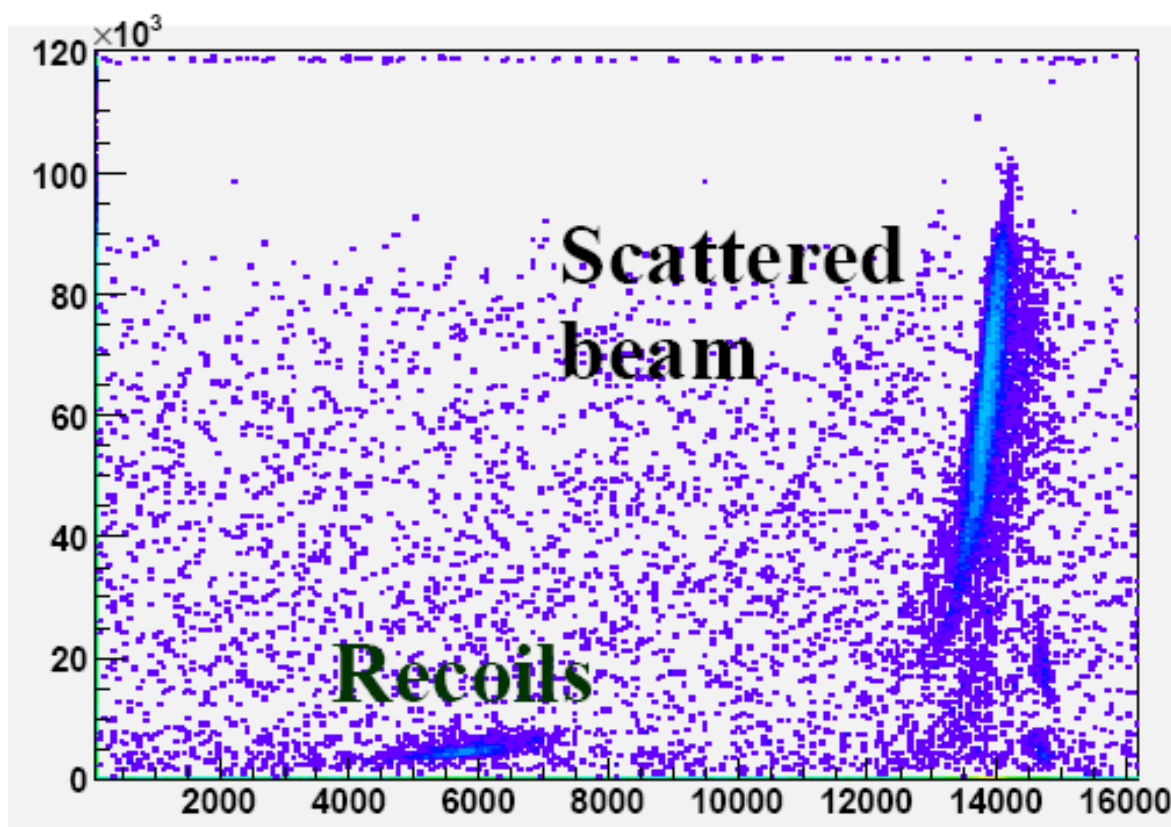


Figure 3: Plot of time of flight versus energy for particles reaching the VAMOS focal plane in the reaction  $^{22}\text{Ne} + ^{197}\text{Au}$ .

Confirmation that the evaporation residues were implanted into the focal plane Si detector was obtained by measuring the  $\alpha$ -particle energy spectrum, which is shown in figure 4. The distribution of  $\alpha$  particles across the strips was analysed and found to be slightly off-centre. This was attributed to an overestimation of the effective Wien filter field length. However, it was believed this could be corrected in future measurements in this separator mode by reducing the Wien filter's magnetic field strength, provided the power supply is capable of allowing precise control and stability at those lower values.



The transmission efficiency was determined from the yield of  $\alpha$  particles using the known cross section, beam dose and target thickness. The deduced value of around 35 % is consistent with optics calculations and is very large compared to other recoil separators for this type of reaction.

The beam suppression factor turned out to be much lower than expected for reasons that are at present not fully understood. One possibility is that a direct beam having different charge states could be responsible for the high counting rates in the Si detector. It is noteworthy that high counting rates have been observed at the focal plane of VAMOS on other experiments using the separator in standard mode, so it does not appear necessarily to be related to the operation of VAMOS in this novel mode. It is clearly not a general problem for Wien filters since devices such as the velocity filter SHIP are routinely able to provide very good beam suppression for asymmetric reactions. Further work is being undertaken to isolate the cause of this effect.

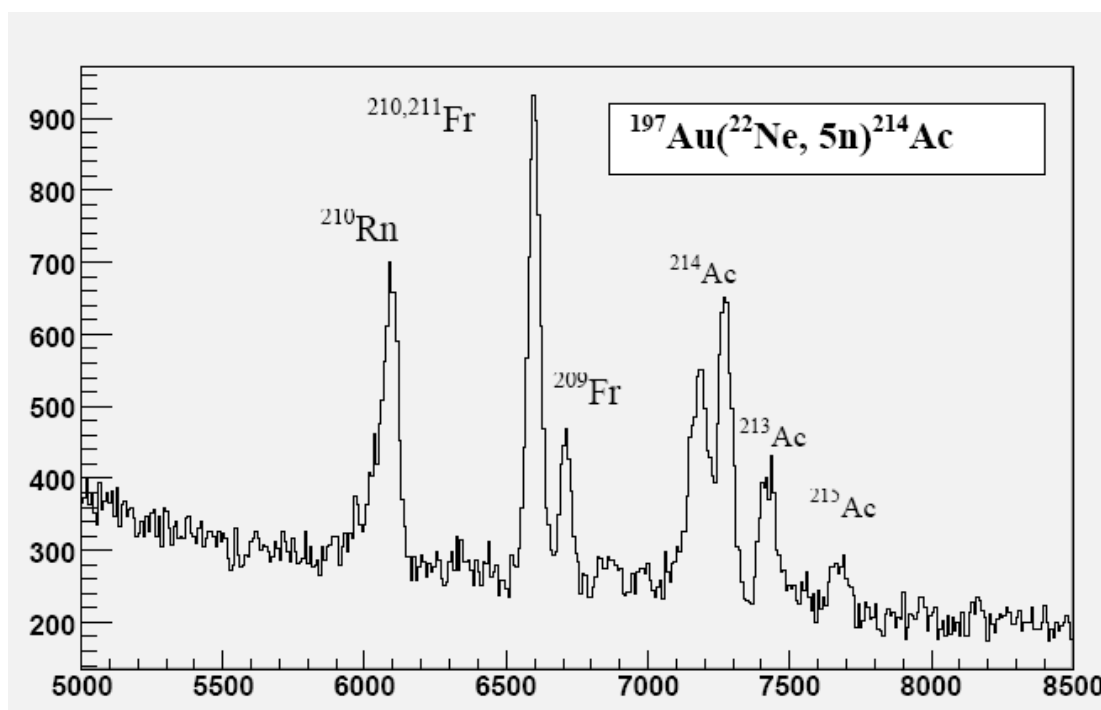


Figure 4: The  $\alpha$ -particle energy spectrum measured in the Si detector at the VAMOS focal plane.

## Conclusions and Future Prospects

The in-beam tests performed using VAMOS in a new mode with the Wien filter set to transmit the beam straight through have demonstrated that it is possible to collect the evaporation residues of interest with high transport efficiency. A programme of investigations is in place to identify and solve the problems with the low beam suppression factor encountered in these tests. These problems are not



thought to be a consequence of using VAMOS in this novel way and are certainly not a general problem for velocity filter devices. It is also worth noting that for the experimental programme proposed for EURISOL employing more symmetric reactions it will be necessary to construct a Wien filter capable of providing greater field strengths than are possible with VAMOS.

### Acknowledgements

The experimental work presented in this report was performed by E519 collaboration at GANIL. The authors of this report would particularly like to thank Ch. Theisen and B. Sulignano.

### Summary of Design Criteria

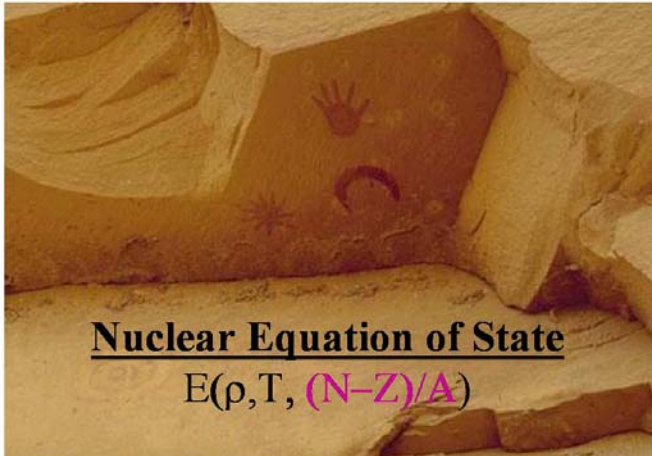
The design criteria that have been specified for the recoil separator for EURISOL are as follows:

- Mass resolution is not essential, as tagging techniques and genetic correlations can be used to identify implanted recoils. It can be useful to obtain a rough (1%) identification of evaporation residues in some SHE synthesis experiments.
- High transmission efficiency is a priority for symmetric, asymmetric and inverse kinematics reactions. The separator should improve on existing devices for reactions such as  $^{48}\text{Ca} + ^{208}\text{Pb}$  (i.e.  $> 40\%$ ).
- A high beam suppression factor  $>10^{12}$  is essential in order to maintain a low counting rate at the focal plane.
- The separator should be able to deal effectively with reactions such as Ca+Pb and Sn+Xe.
- The momentum acceptance should be larger than 12% to preserve a good transmission for very asymmetric reactions.
- The angular acceptance should be larger than  $\pm 5$  degrees.
- The focal plane image size should be compact to allow the addition of Ge and Si detectors in close geometry.



# In-beam Validation of the FAZIA Design Concept for EURISOL

## Physics Motivation



A new high-performance RIB facility like EURISOL will offer the possibility to study the role of the isospin ( $N/Z$  ratio) in dynamical and statistical de-excitations of hot nuclei produced in central and peripheral collisions [1-3].

This search will probe the dependence of the nuclear equation of state (EOS) on the isospin terms under compressed, normal and dilute conditions. We recall that, apart from the astrophysical interest, the knowledge of the isospin dependence of effective interactions in regions far

away from saturation is of great importance for nuclear structure studies of exotic nuclei. Properties of the liquid-gas phase transition for hot nuclei with large  $N/Z$  ratios will also place decisive constraints on the phase diagram. Moreover, a hot nucleus for which one can vary the two fermionic components is a unique laboratory for statistical physics of mesoscopic systems. The study of collective flows will give complementary information with respect to the analysis of isospin effects on the multifragmentation dynamics.

## Outline of Challenges and Conceptual Solution

From an experimental point of view, to exploit fully Radioactive Nuclear Beams facilities and study the effects of large isospin variation, it is necessary to identify both the  $Z$  and  $A$  of particles and fragments over the largest possible ranges. The present identification techniques (Time of Flight, Telescope  $\Delta E-E$ ) do not allow the identification requirement to be fulfilled over a large dynamic range. Several multi-detector systems are currently being intensively exploited at European nuclear physics facilities and are generating major advances in the scientific fields described above. For the study of nuclear dynamics and thermodynamics, current state of the art arrays include INDRA (1993, France) and CHIMERA (1999, Italy). At present, experimental results from INDRA and CHIMERA collaborations are considered as the reference in the worldwide competition. But mass and charge identification are currently very limited for both apparatus. To fully benefit from radioactive beams, complete identification



is necessary up to  $A \sim 50$ . This will only be achievable through the development of Pulse Shape Discrimination (PSD) techniques and the corresponding electronics.

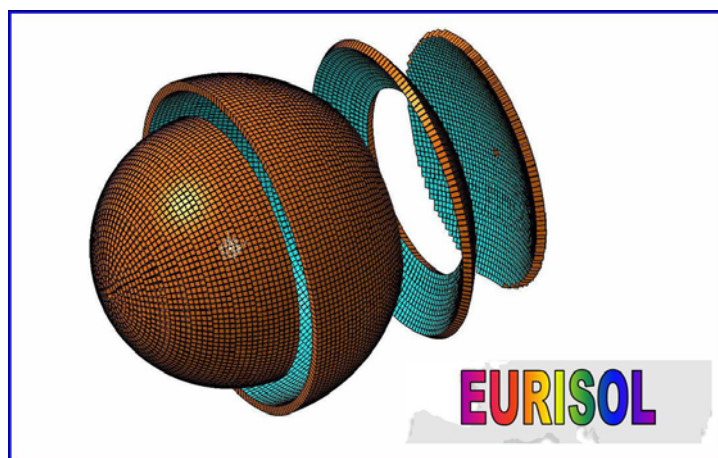


Figure 1: Schematic view of the FAZIA design concept for EURISOL.

Mass and charge identification is one of the major challenges of particle detection systems. At present, two techniques are generally employed: time of flight and energy loss measurements. The former requires long flight paths which translate into large, expensive and somewhat cumbersome arrays. The latter implies high thresholds which preclude the identification of important low energy particles. More recently, particle identification through pulse shape analysis has been proposed and promising preliminary studies have been performed. The combination of the three techniques should open a path towards more compact and efficient arrays. We intensively investigate the potential of mass and charge discrimination through pulse shape analysis in both silicon and CsI detectors. Research in this area includes development of electronics (signal digitization), algorithms and materials (e.g., neutron transmutation doped silicon).

The main challenges in the case of nuclear physics stem from the large energy ranges of the particles detected. We are concentrating on the development of front-end, timing and shaping electronics having the required high dynamic range.

The detection array has to be compact and simple, in order to cover the whole solid angle. The number of detectors needed has to be sufficiently large to obtain a precise determination of the characteristics of the charged products emitted in the reaction, with special regard to the precision in the emission angle. Compact electronics has to be associated with an analogue and a digital part. The analogue part will allow a first (low-noise, high dynamic range) pre-amplification of the signal. The digital part will sample the signal and perform the pulse shape analysis on-line with a fast digital signal processor with subsequent recording of the results of the detection.



## Time scale and step policy

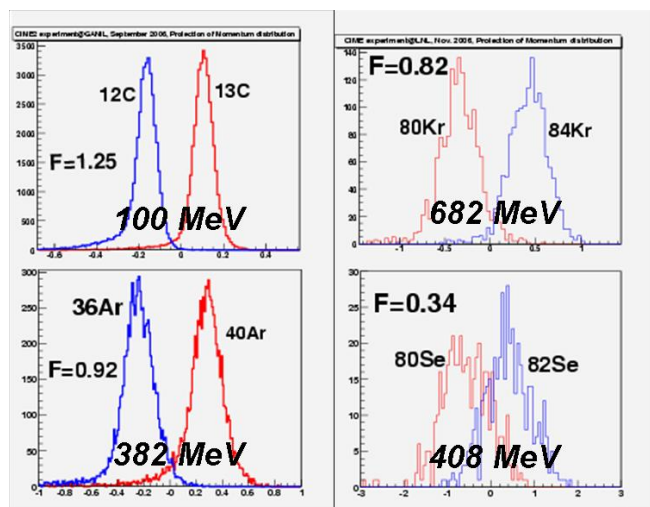
The basic idea is to develop a detector array in 4 steps:

1. FAZIA *Prototype phase* to define the basic telescope cell.
2. FAZIA *Prototype-array phase*: on the basis of the conclusion drawn in the preceding phase, design and construction of a prototype array (it will consist of about 20-30 basic telescope cells arranged in an array geometry which fulfil technical needs in terms of granularity and angular resolution for test of mechanical problems, cross-talk, DAQ, etc...).
3. FAZIA-Array for *SPIRAL2*: construction of a FAZIA array appropriate for SPIRAL2 beams with large solid angle coverage.
4. Final  $4\pi$  FAZIA-array for EURISOL.

The completion dates are 2008 for step 1, 2010 for step 2, 2012 for step 3 and 2015 for the final FAZIA array.

## Experimental Details of Validation Tests

In the high-energy configuration of the FAZIA prototypes, each telescope includes three elements: Si-Si-CsI(Tl). The first two Si elements act as a high-resolution telescope. Both detectors are mounted in the reverse-field configuration. The reverse-field configuration of the first element permits PSA with very low thresholds, while the reverse-field configuration in the second, thicker Si detector provides a redundant PSA and the implementation, together with the third element CsI(Tl), of an original Si-CsI(Tl)  $\Delta E$ -E configuration, called Single Chip [4] where the Si detector acts both as a standard semiconductor detector and as a photodiode to catch the CsI(Tl) fluorescence.



A series of implantations of ions with fixed energy, known charge and known mass has been performed to study the response of the silicon (Tandem ORSAY, GANIL and LNL, see for example [14]). The feasibility of the discrimination technique was demonstrated (see Fig. 2).

Figure 2: Identification methods for ions stopped in one silicon detector analysing the shape of the current signal ( $F$ =factor of merit).



FAZIA is characterized by a fully digital implementation, except for the preamplifiers, which nevertheless present original solutions. In fact, the silicon detectors are coupled to preamplifiers able to produce charge and current outputs (PACI, [7]). These outputs are digitized by fast ADCs. The MAR ASIC analogue memory digitizer developed within FAZIA (able to convert at 2 GSamples/s with 12 bits) is used to sample the current and compared with commercial state-of-the-art digitizers. The digitized signals are processed in order to extract all the relevant information: energy, timing, Pulse Shape (i.e. Z, A) [5,7].

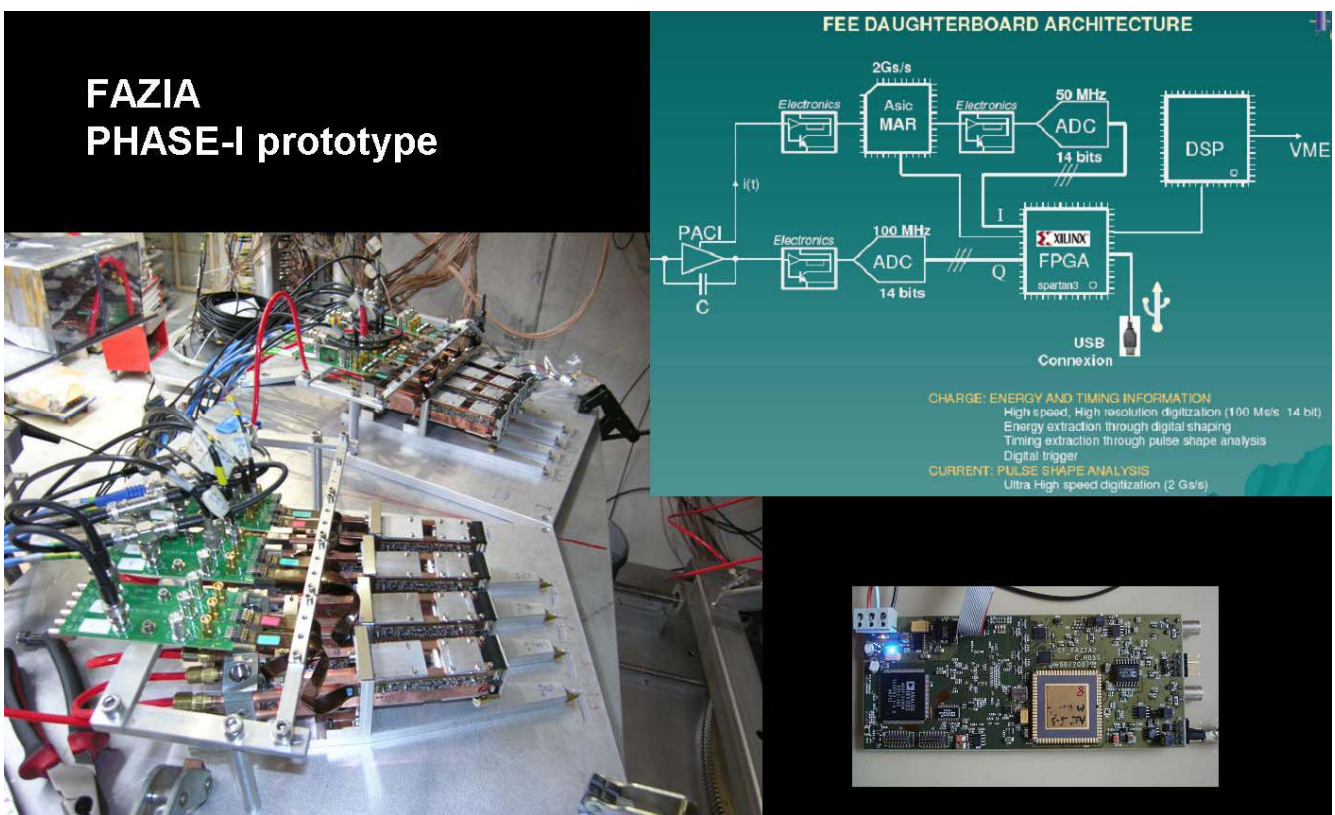


Figure 3: R&D FAZIA (prototype phase): prototypes and Front End Electronics.

The Phase 1 Front End Electronics is shown in Fig. 3-right, while Fig. 3-left shows the mechanical supports for the telescopes which have been built and already used for tests with low energy beams at LNL (Legnaro). Further tests with high energy beams are scheduled in 2009 in GANIL and LNS (Catania).

As far as silicon detectors are concerned, they are mounted in the so called “reverse-side”



configuration [9], presently believed to be the best suited for optimizing the Pulse Shape performances. Mono-energetic ions produced in GANIL were stopped in silicon-detectors to test the two configurations: (i) ions are entering from the high field side (“direct or front side configuration”) or (ii) ions are entering from the low field side (“inverse or reverse configuration”) (see Fig. 4).

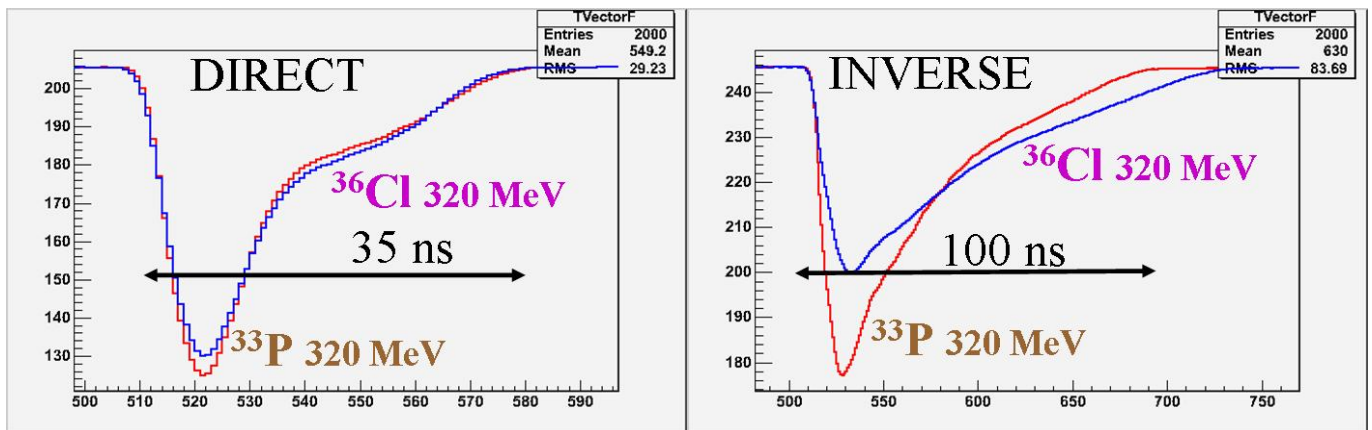


Figure 4 (data from FAZIA-GANIL experiment): mean current signals (from about 100 signals) for different ions stopped in silicon-detector.

The “front-side” configuration is expected to perform better in terms of timing [10]. The two alternative solutions will be compared in 2009. The Single Chip read-out [4] is based on the idea of using the silicon detector to act both as ionization detector element and as a photodiode to read the fluorescence of the CsI(Tl). It has already shown good performance in preliminary tests in LNL and will also be checked as a realistic and large-scale alternative to the standard solution in 2009.

Presently we use 20x20mm silicon detectors built by FBK-Trento and Canberra, starting from silicon wafers provided by the FAZIA collaboration, i.e. wafers obtained by a special “random orientation” cut, starting from a  $\langle 100 \rangle$  nTD silicon ingot from TopSil.

In fact, from a series of experiments [11,12] performed with stopped ions at LNL, we learned that this procedure guarantees the best performances because it maximally reduces the “channelling” (i.e. crystal orientation) effects in the silicon crystal. As an example, the left panel of Fig. 5 shows the current signals obtained during an experiment at LNL with Se beam, when the 300  $\mu\text{m}$  thick silicon detector was oriented perpendicular to the scattered particles (thus entering along the  $\langle 100 \rangle$  axis), while the right side shows the same signals when the silicon detector was oriented in the “non-channelled”, i.e. “random” direction. The improvement in the stability of the current signals is apparent.

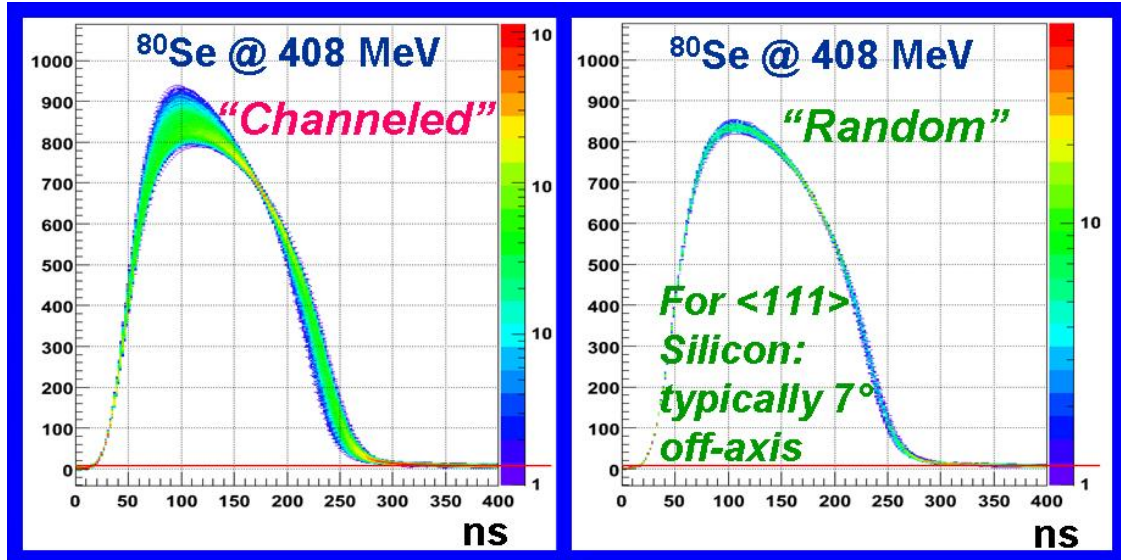


Figure 5 (data from FAZIA-LNL experiment): Current signals for channelled (left panel) and “random” (right) entering ions. Elastic scattering of 408 MeV  $^{80}\text{Se}$ . Ions are stopped in the Si detector.

The mechanics of the Phase 1 telescopes is equipped with various angular degrees of freedom, in order to be able to test also other detectors and different silicon wafer cuts (Fig. 6).

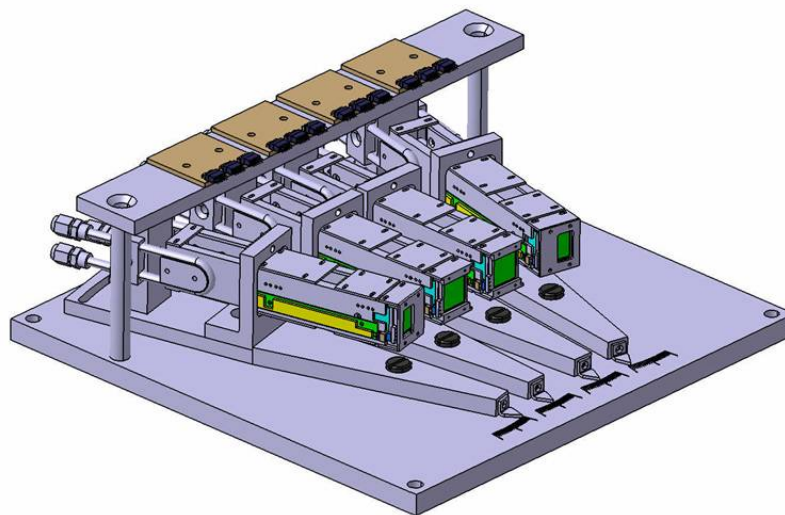


Figure 6: Telescope and mechanical support (FAZIA-Phase 1).



The Si detectors are all of the “nTD” kind, having average resistivity of about  $3\text{k}\Omega\cdot\text{cm}$ ; they have been characterized in terms of resistivity uniformity, which is indeed a very critical parameter for getting the necessary Pulse Shape Analysis (PSA) resolution. Typical off-the-shelf detectors have resistivity uniformity of 10% or larger, while we estimate that the present application requires uniformity at least a factor of five better.

The resistivity uniformity test has been performed using a technique based on pulsed-laser irradiation of the detectors developed by the collaboration [13]. Measured maps of two detectors are shown in Fig. 7. On the left side a detector with typical resistivity non-uniformity around 10% is presented, showing the residual circular striations, remnants of the original Float Zone processing. A significantly better uniformity (around 1%) characterizes the detector on the right side.

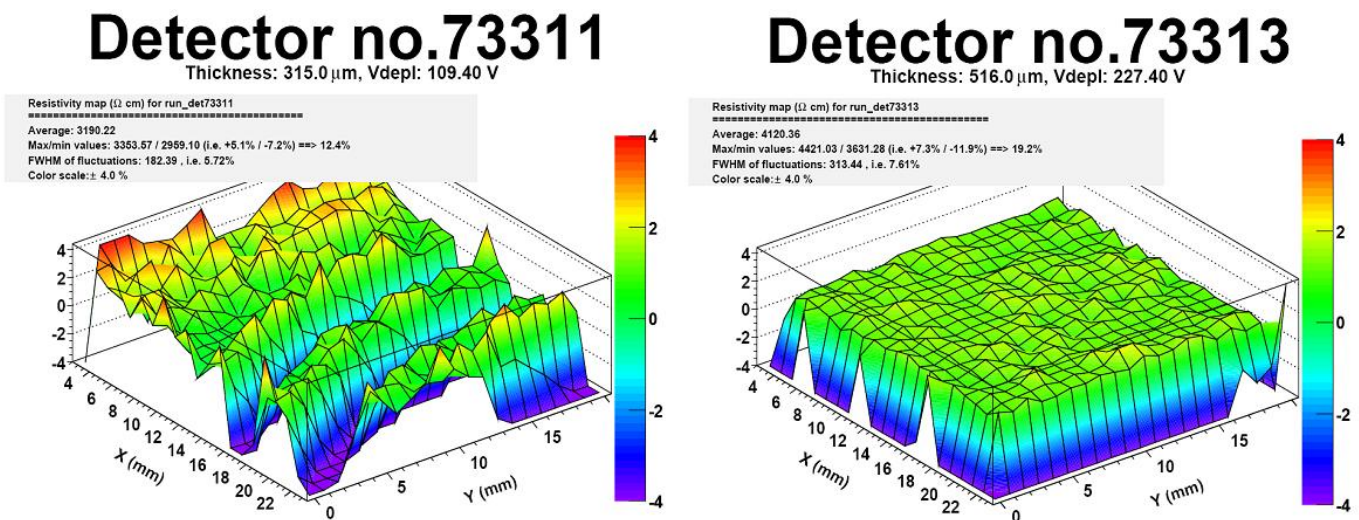


Figure 7: Experimental maps of resistivity (doping uniformity) of two nTD-silicon detectors of the FAZIA project. On the left-side a detector with “typical” uniformity around 10% is shown. On the right-side a detector with 1.5% uniformity is shown.

The experience gained within the FAZIA collaboration about the silicon material (channelling and homogeneity) and digital signal processing has led to progress in the field of PSA in silicon. As an example, Fig. 8 shows the recent results obtained at LNL, using the reaction  $^{32}\text{S} + ^{27}\text{Al}$  at beam energy of 474 MeV. Beyond charge separation, clear mass identification is observed for a significant energy range, for many elements. The full energy scale of the system was 1.3 GeV.

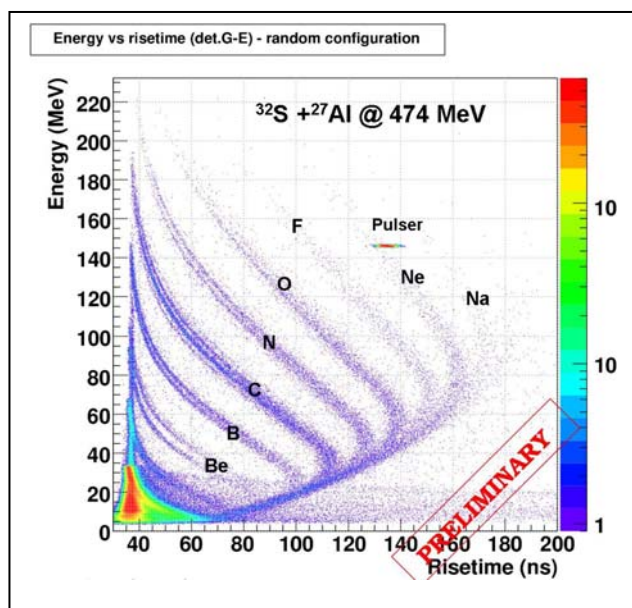


Figure 8: The energy vs. risetime (charge signal) obtained from a 500 $\mu$ m detector, having a 1.5% resistivity uniformity and oriented in such a way to avoid “crystal orientation effects”.

This standard plot [9] is one of the many correlations that can be used for particle identification and that are under study. These data (and some other similar results involving both charge and current information) show unprecedented identification quality by means of PSA using digital sampling techniques.

## Future Plans

The maximum available energies and the limited Z range explored in LNL did not permit the very limit of the proposed approach to be determined. Experiments at LNS and GANIL in 2009 will be of paramount importance to determine ranges and thresholds for the Z and A identification in our approach over a much broader range of energies. In experiments in 2009 we also plan to test a novel system for measuring Time of Flight based on synchronization of the detectors via an analogue periodic signal and the use of flashes of light [6]. The issue of rear/front injection will also be addressed, with the main goal of determining in a sound and reproducible way the energy thresholds of the two approaches. The associated issue of timing performances will also be addressed. The issue of radiation damage and associated possible PSA degradation by studying the performances of a selected detector as a function of the total flux of elastically scattered (and implanted/ not implanted ions) will also be studied in 2009.

## REFERENCES

- [1] Web site Fazia collaboration (<http://fazia.in2p3.fr>)
- [2] LOI-SPIRAL2, Dynamics & Thermodynamics of exotic nuclear systems
- [3] “Dynamics and thermodynamics with nucleonic degrees of freedom”, W.Trautmann et al. eds, Springer 2006.
- [4] G.Pasquali et al, NIM A301 (1991) 101



- [5] L.Bardelli et al, NIMA 521 (2004) 480
- [6] L.Bardelli et.al, NIMA 572 (2007) 882
- [7] H.Hamrita et al NIMA 531 (2004) 607 and PhD thesis,tel-00010145
- [8] L.Bardelli, G.Poggi NIMA 560 (2006) 517
- [9] M.Mutterer et al, IEEE Trans. Nucl. Science 47 n.3 (2000), 756
- [10] Chimera collaboration, see for example G.Politi at al, Proceedings of IWM2005, 28 November 2007, Catania, Italy
- [11] L.Bardelli, Laboratori Nazionali di Legnaro (LNL) Annual Report 2006
- [12] L.Bardelli, Proceedings of IWM2007, 4-7th November 2007, Ganil, France,
- [13] L.Bardelli et al., in preparation
- [14] S.Barlina et al., submitted to NIM A



## Direct Reactions at EURISOL: In-beam tests to validate the design of an array for light charged-particle and gamma-ray measurements.

### Physics Motivation

The study of the shell structure of exotic nuclei is one of the fundamental keys to understanding the nuclear many-body system. Experimental results around the  $N=20$  and  $N=28$  shell closures have confirmed a variation of the shell ordering as the neutron to proton ratio increases. Direct reactions are one of the most suitable tools to probe the single-particle structure of radioactive nuclei. Beams of neutron-rich nuclei will be available at EURISOL at reasonable intensities allowing these studies to be expanded to unexplored regions of the nuclear chart.

The wide physics case described as part of the direct reactions studies within the EURISOL scientific programme [1] requires the common design of a system that combines high efficient gamma-ray and charged-particle detection. This system should be suitable for operation in conjunction with arrays of neutron detectors, recoil spectrometers to identify heavy fragments and cryogenic or polarized targets. This report will summarize the main technical requirements for the design and will present preliminary results from some in-beam tests.

### Conceptual Design and Technical Requirements

Direct reactions performed in inverse kinematics will require the detection of light charged particles, gamma rays and neutrons in combination with a spectrometer for the beam-like particles. The charged particle detector array should identify the  $Z$  and  $A$  of each particle detected, measure the particle energies and the angles at which the particles are emitted. The charged particles will generally have low values of  $Z$  and  $A$ , so the  $\Delta E$ - $E$  method using silicon detector telescopes and the time of flight method are proposed for particle identification. Silicon strip detectors with an appropriate degree of segmentation can provide the required angular information and measure the particle energies with reasonable precision, provided the target thickness is not too great. Higher-energy particles could penetrate through the Si detectors, so an outer layer of scintillating material, similar to that proposed for FAZIA and already used



in some current arrays, will be used to stop the particles completely.

Monte Carlo simulations of experiments of this type have been performed and clearly demonstrate that the target thickness is a key factor in determining the energy resolution that can be achieved with the charged particle array. For reactions populating excited states, the detection of gamma rays can be used to determine the excitation energies of states with much greater precision. The efficiency of the gamma-ray detector array has to be as high as possible to allow the most exotic nuclei to be investigated. Possible solutions for the gamma-ray array include the  $4\pi$  AGATA spectrometer based on germanium detectors and arrays of scintillator detectors made of materials such as caesium iodide or lanthanum halides. AGATA should give excellent energy resolution and allow corrections for Doppler broadening to be made. A scintillator detector array could provide a higher efficiency, although the energy resolution would be worse. The choice could depend on the particular nuclei under study.

In this report we present results obtained by coupling two state-of-the-art charged particle detector arrays (TIARA and MUST2) with EXOGAM germanium detectors and the VAMOS recoil separator. The results demonstrate the feasibility of performing experiments with low-intensity beams, as might be expected for the most exotic nuclei with EURISOL. In particular, spectra have been obtained by requiring triple coincidences between charged particles, gamma rays and beam-like particles. The experimental spectra from the charged particle detector arrays are also compared with Monte Carlo simulations.

### In-beam tests and validation of simulations

A campaign of experiments using a combined detection system of silicon and germanium arrays was carried out at SPIRAL/GANIL in 2007, allowing the design choices proposed for EURISOL to be validated. The experimental setup comprised the MUST2 silicon array at forward angles (0-30°) coupled to the TIARA barrel and the Hyball at angles (35-180°). This composite array covered a large fraction of  $4\pi$  solid angle for the charged particles (see Fig. 1). The EXOGAM germanium array was placed at 5 cm distance to the target to enhance the gamma-ray efficiency. In addition the large acceptance spectrometer VAMOS was used to select the beam-like particles providing a full kinematic identification of the reaction channel. This setup represents a large step forward to an integrated particle-gamma array and the results will certainly be a benchmark for future design.



Two experiments were carried out using  $^{20}\text{O}$  and  $^{26}\text{Ne}$  SPIRAL beams aimed at studying the shell structure of exotic nuclei at the  $N=16$  shell gap. The experimental conditions in terms of beam intensity were to some extent different. While the  $^{20}\text{O}$  beam was provided by the SPIRAL facility with an intensity of  $10^4$ pps, the  $^{26}\text{Ne}$  beam had only 1000 pps. The  $^{26}\text{Ne}$  intensity required the use of a deuterated polyethylene target that was twice as thick ( $1\text{mg}/\text{cm}^2$ ) as the one used in the  $^{20}\text{O}$  experiment to partially compensate for the lower beam intensity.

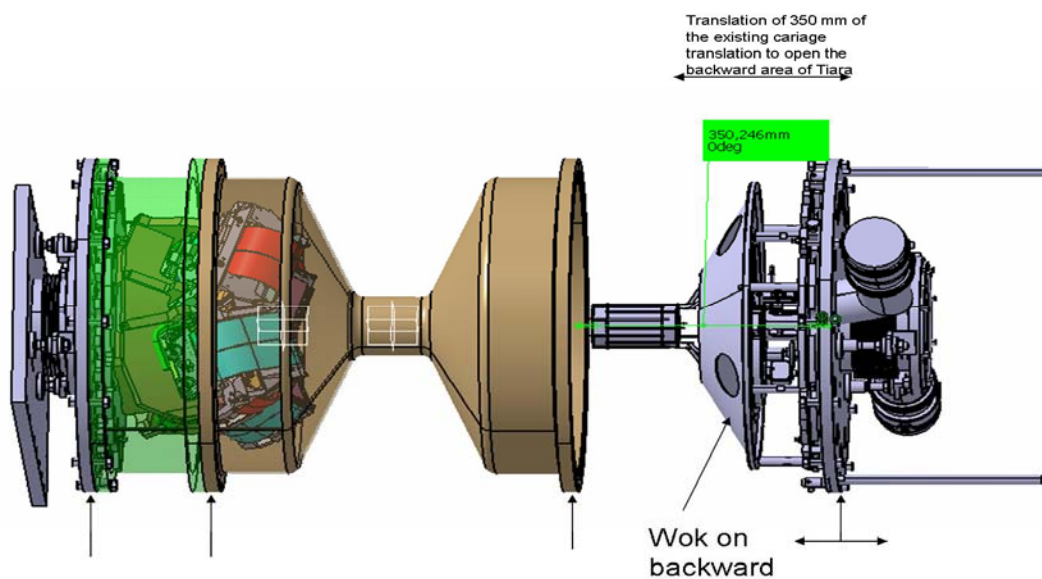


Figure 1: Coupling of MUST2 and TIARA silicon arrays.

## Results

In this section preliminary results from the first experiment will be presented. The identification matrix ( $\Delta E$ - $E$ ) of the beam-like particles obtained from the VAMOS focal plane detection system is presented in Fig. 2 a). The plot shows different isotopes of oxygen produced in the reaction. Results of the energy-angle correlations obtained by gating on  $^{21}\text{O}$  are presented in Fig 2 b). The angular distributions show the first evidence of the ground state and the first excited states at roughly 1.28 MeV.

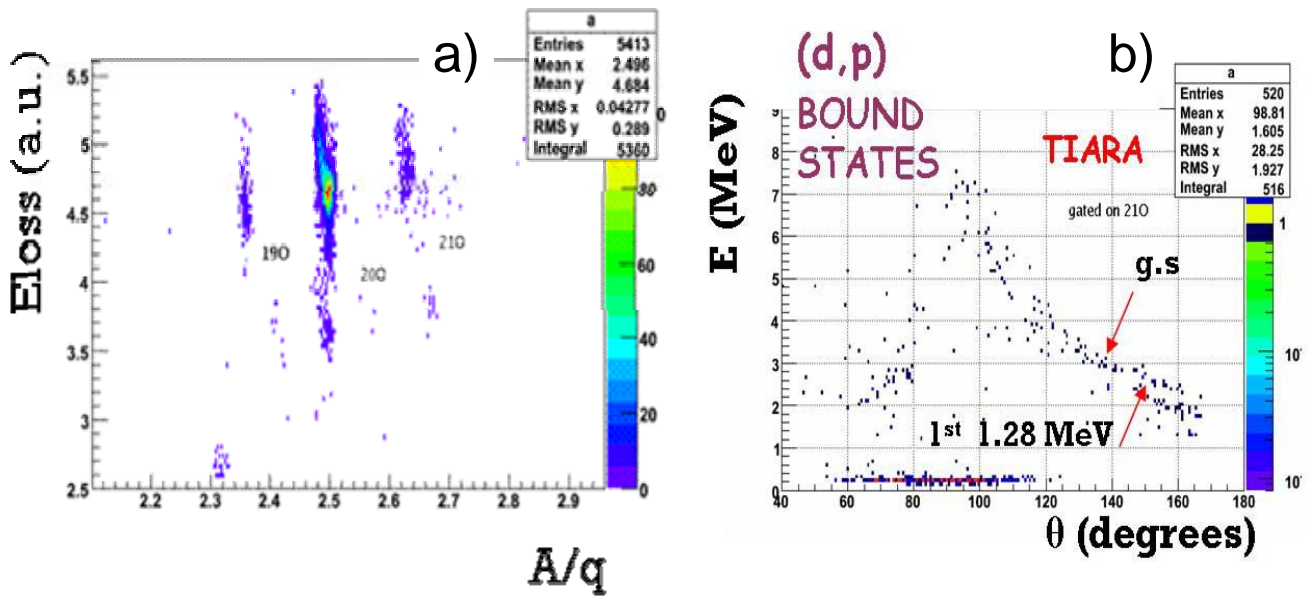


Figure 2: a) Identification matrix obtained from VAMOS b) Energy-angle correlations obtained in TIARA when gating on  $^{21}\text{O}$ .

In addition, some other channels of the reaction such as (d,t), (d,d), (d,d') have been recorded simultaneously with MUST2 and TIARA, confirming the enormous potential of this setup. The energy-angle correlations for the (d,t) channel obtained when gating on  $^{19}\text{O}$  are presented in Fig. 3 [A. Ramus Ph. D. thesis IPN Orsay].

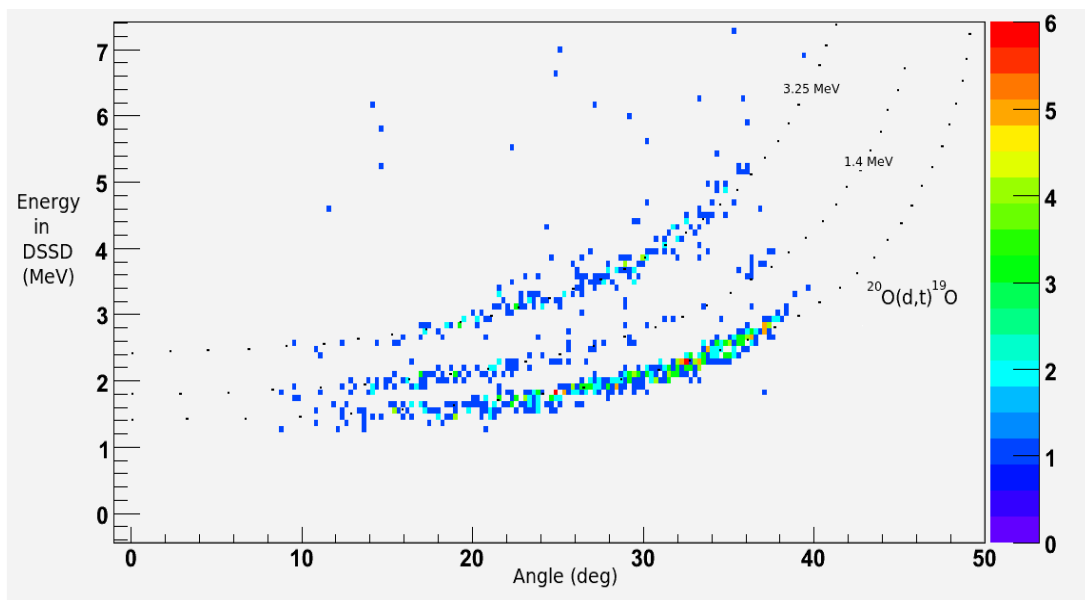


Figure 3: Energy-angle correlations for the (d,t) channel obtained in MUST2.



As well as measuring transfer to bound states, the experimental setup allows the transfer to unbound states to be measured owing to the large acceptance of VAMOS. When transferring a neutron to an unbound state the recoil  $^{21}\text{O}$  breaks immediately at the target reaching the focal plane as  $^{20}\text{O}$ . By gating on  $^{20}\text{O}$  (see Fig. 2 a)) we can distinguish two groups in Fig. 4: one at approximately  $\theta_{\text{lab}} \sim 70^\circ$  coming from the elastic and inelastic scattering and the second, between  $\theta_{\text{lab}} \sim 70^\circ$  and  $130^\circ$  enclosed by the polygon, arising from the transfer to an unbound state at roughly 5 MeV.

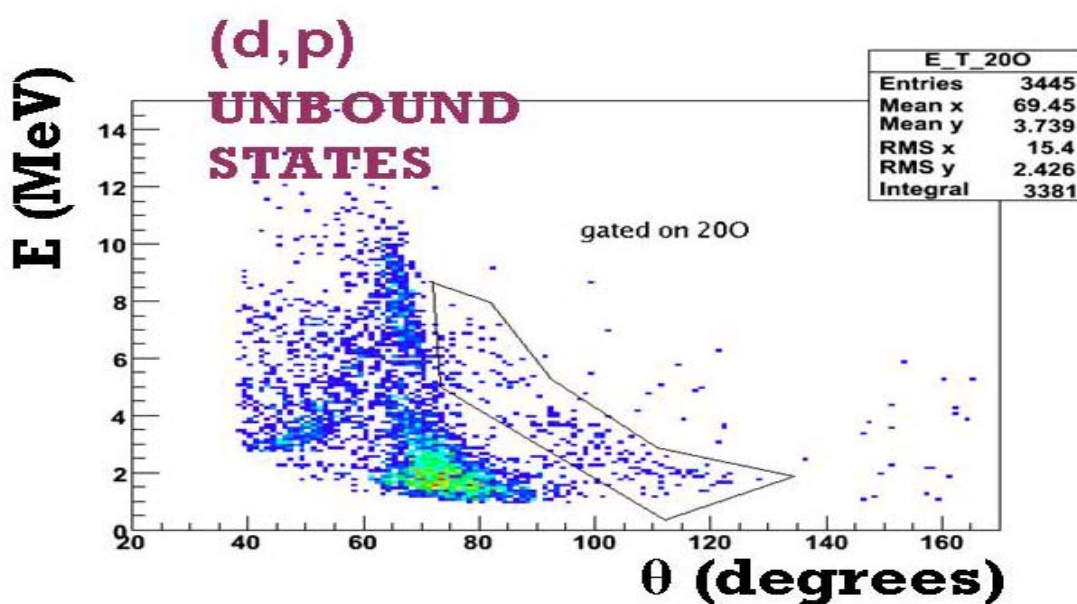


Figure 4: Energy-angle correlation obtained in TIARA when gating on  $^{20}\text{O}$

The triple coincidences (beam-like particle + ejectile + gamma ray) are shown in Figure 5. The first excited state of  $^{20}\text{O}$  at  $\sim 1.7$  MeV can be resolved with good efficiency ( $\sim 10\%$ ) and reasonable resolution ( $< 100$  keV). This represents one of the most relevant outcomes for the design of the integrated particle-gamma array. In addition, simulations of the experimental setup were also performed and excellent agreement between the experimental results and the simulations has been found.

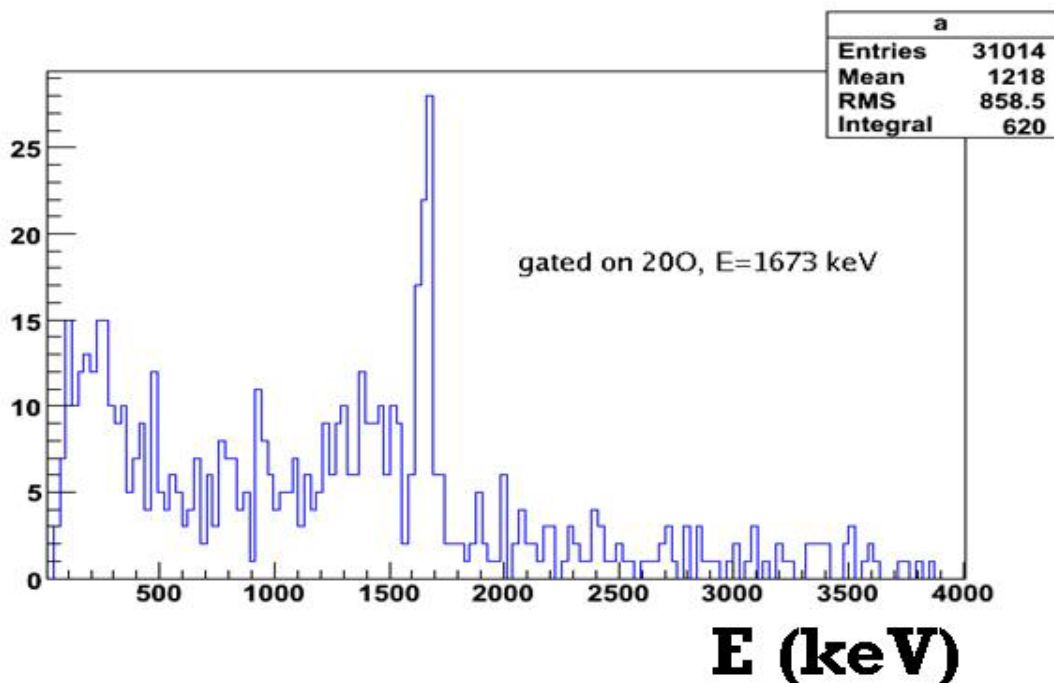


Figure 5: Gamma-ray energy spectrum measured using EXOGAM obtained by gating on  $^{20}\text{O}$  and requiring triple coincidences of charged particles in TIARA or MUST2, gamma rays and beam-like particles.

### Simulations of the $^{20}\text{O}$ experiment

The full setup geometry has been implemented in the GEANT4 simulation toolkit (see Fig 6 a)) and the experimental results obtained during this campaign have been used to validate the simulations. Fig. 6 b) shows the simulated energy-angle correlation obtained in TIARA for the transfer to the bound states of  $^{21}\text{O}$ . The simulated spectrum matches the experimental data perfectly (see Fig. 2 b)) [S. Brown Ph.D. thesis Surrey University]. This excellent agreement allows this simulation tool to be used with confidence for simulating more optimal gamma-particle array designs and reactions studying states in more exotic nuclei, such as  $^{24}\text{O}$  or  $^{133}\text{Sn}$ .

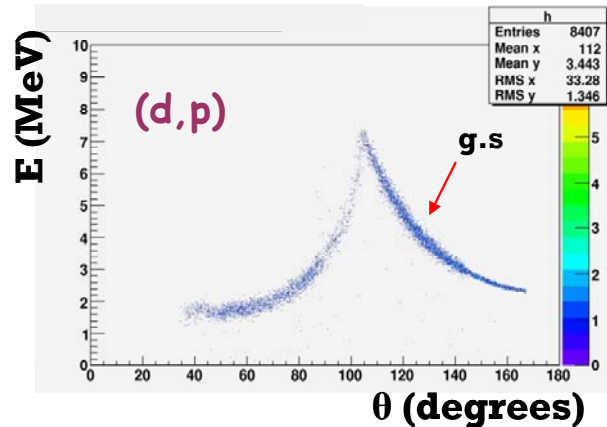
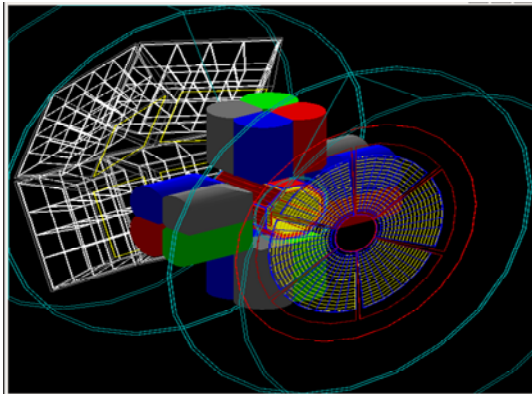


Figure 6: a) Geant4 simulation of the  $\gamma$ -particle array: TIARA barrel + TIARA hyball +MUST2 +EXOGAM b) Simulations of the energy-angle correlations obtained in TIARA for the ground state.

## Conclusions and Future Prospects

Simulations reproduce the response of arrays and give an insight into the main parameters that contribute to performance. Preliminary analysis of the validation experiment confirms that we can study different reactions channels, obtain level energies and l-value information. In particular, it was possible

- To observe transfer to bound and unbound states with full channel identification
- To obtain triple coincidences with excellent gamma energy resolution
- To acquire (d,d') and (d,t) data simultaneously with TIARA and MUST2
- To include unbound states exploiting the large angular and momentum acceptance of VAMOS

## Acknowledgements

The author wishes to acknowledge the collaborations E522S and E445S involved in the experimental campaign.



# In-beam validation of the Paul trapping of low energy radioactive ions and direct detection of the beta-decay

## Physics Motivation

Atom and ion traps have found a wide range of applications in nuclear physics for the confinement of radioactive species. In particular, the continuous improvements in magneto-optical trapping efficiencies achieved over the last ten years or more have resulted in a number of precision measurements for the study of fundamental interactions, as well as for the determination of nuclear static properties. The environment offered by traps in beta-decay measurements is ideal for reducing instrumental effects like electron scattering in matter, or for enabling the direct detection of recoiling ions. Such conditions have led to measurements of angular correlation coefficients in beta decay with unprecedented precision, motivated by the search for exotic interactions as signatures of physics beyond the standard electroweak model.

## Outline of Challenges and Conceptual Solution

Although the principles of ion trapping were established well before those of magneto-optical confinement, the application of ion traps for beta decay experiments with radioactive species is more recent. Technically, magneto-optical traps (MOTs) are often limited to alkali elements, for which suitable lasers can be found. They enable the preparation of samples of smaller size and with atoms at lower energies than ion traps. Elaborate transition schemes have recently been applied to radioactive He atoms. However, the efficiencies achieved so far with noble gas atoms in MOTs are still too small for practicable precision measurements of beta decay correlations.

Another consideration is that the standard geometry of a 3D Paul trap, in which the hyperbolic electrodes are made of solid material, is not well suited for the detection of decay products following beta decay. Ion confinement of radioactive species requires, in addition, beam preparation for efficient



trapping and such techniques pose new challenges when applied to light mass species.

This has motivated the adaption of the Paul trapping technique in order to confine abundant quantities of radioactive ions and furthermore be able to observe their beta decay directly. The concept is based on a novel transparent Paul trap made out of coaxial rings and surrounded by suitable detectors. Besides the study of fundamental interactions in nuclei, such a scheme opens also the possibility of new trap assisted decay experiments that will form an important part of the EURISOL physics programme.

### Experimental Details of Validation Tests

The experiment was carried out at the new low energy beam line LIRAT of the SPIRAL facility at GANIL. A first test was performed in 2005 during the commissioning of the LPCTrap facility but the performance observed in that first run was not sufficient for practicable beta-decay measurements using traps. This validation test was performed using  ${}^6\text{He}^+$  ions produced by the SPIRAL ECR source.

The setup for the beam preparation (Fig. 1) comprises a radio frequency quadrupole cooler and buncher (RFQCB) followed by two pulsed electrodes located before the Paul trap. The beam intensity at the entrance of the RFQCB was typically 10nA, including the contribution of the stable  ${}^{12}\text{C}^{2+}$  ions. Under optimal conditions, the  ${}^6\text{He}^+$  beam intensity at the entrance of the RFQCB was  $2 \times 10^8$  pps.

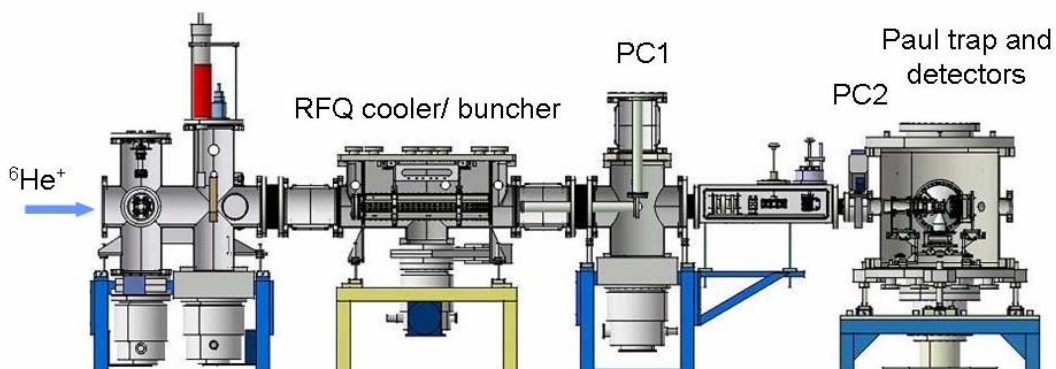


Figure 1: General layout of the setup for the preparation of the low energy beam.



The beam was cooled in the RFQCB using the buffer gas technique, which is relatively fast and universal, and well suited for radioactive species. Since the cooling is only efficient at energies of about 100 eV, the RFQCB is mounted on a high-voltage platform, operated 100 V below the voltage of the ECR source platform which was set at 10 kV. In the RFQCB, the ions are confined radially by an RF field applied to four cylindrical rods. The rods are segmented in order to generate a longitudinal electrostatic field which drives the ions toward the exit of the structure. Inside the cooler, the ions are accumulated to produce a bunch for efficient injection into the Paul trap. The bunch is extracted from the RFQCB by fast switching of the buncher electrodes after thermalization of ions with the H<sub>2</sub> buffer gas.

The ions are then transported through a first pulsed cavity (PC1) followed by an electrostatic lens and finally through a second pulsed cavity (PC2) before their injection into the Paul trap. Switching voltages applied to PC1 and PC2 reduce the mean ion energies from 9.9 keV to 1 keV and then from 1 keV to 100 eV, respectively, in order to achieve an efficient capture of the ion bunch by the Paul trap.

The ion bunches were injected into the Paul trap at a repetition rate of 10 Hz. The details of this region of the trap are shown in Fig. 2. The electric field inside the trap is generated by two pairs of coaxial rings separated by 10 mm. The frequency used in the trap was 1.15 MHz for a 130 V peak-to-peak voltage amplitude. The RF voltage is applied on the two inner rings whereas the outer rings are grounded. The RF signal on the trap was continuously applied during the measuring cycles. Considering the duty cycle used for the injection of the <sup>6</sup>He<sup>+</sup> bunches into the trap, the beam preparation efficiency was estimated to be  $7 \times 10^{-5}$ , including the deceleration, cooling, bunching, transmission through the pulsed cavities and trapping.

The trap geometry allows the application of suitable voltages on the rings for the injection and extraction of ions. The absence of a massive ring electrode also enables the direct detection of products from decays in the trap. The trap is surrounded by an electron telescope detector and by two ion detectors (Fig. 2). Collimators located in front of the detectors enable the selection of events originating mainly in the trap.

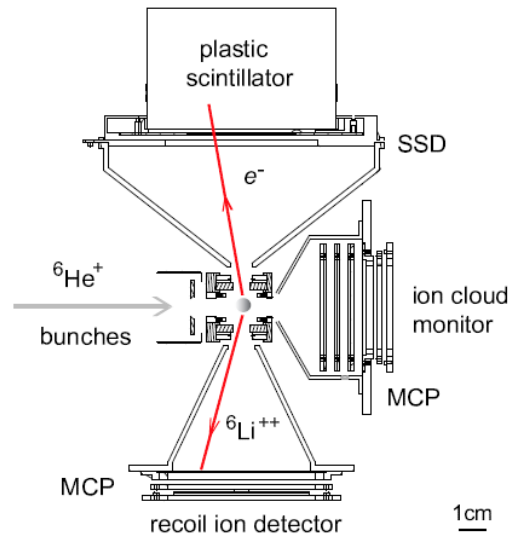


Figure 2: Details of the transparent Paul trap surrounded by suitable counters to detect the products from the beta decay of ions in the trap.

The number of trapped ions was continuously monitored by counting the ions remaining in the trap after a fixed storage time, using the micro-channel plate (MCP) detector located downstream. This detector is preceded by three grids to reduce the intensity of the incident ion bunches. The measured time-of-flight distribution contained a single peak corresponding to a mass-to-charge ratio  $Q/A = 6$ . The storage time of ions in the trap, deduced from the rate of coincidence events and accounting for the beta decay, was 240 ms for a typical pressure in the trap chamber of  $2 \times 10^{-6}$  mbar due to  $H_2$  gas leaking from the RFQCB.

The telescope for beta particles is composed of a double-sided position sensitive silicon strip detector (SSD), with  $2 \times 60$  strips for horizontal and vertical location. The SSD is followed by a plastic scintillator. The recoil ion detector uses two MCPs with delay-line readout providing position sensitivity. The time resolution of the detector is better than 200 ps. An acceleration voltage was applied on an electrode located 6 mm in front of the MCP. The ion detection efficiency reaches 53% for post-accelerating voltages larger than 4 kV.



## Results

A clean signature of in-trap decays can be obtained from the measurement of the beta particle and the daughter recoiling ion in coincidence. The complete kinematics of the decay can be reconstructed from the position information of both detectors, from the measurement of the beta-particle energy, and of the ion time-of-flight relative to the beta particle. The determination of the anti-neutrino rest mass from such a reconstruction provides a useful control to identify background sources and to quantify the signal-to-background ratio. Figure 3 shows such a reconstruction along with the results from a Monte-Carlo simulation.

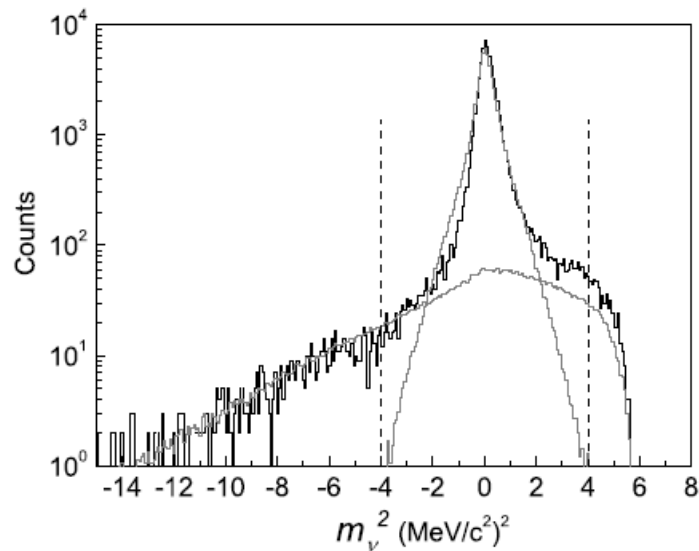


Figure 3: Anti-neutrino rest mass spectrum reconstructed from the decay kinematics (black) and compared with results from Monte-Carlo simulations (grey). The main peak corresponds to decay events occurring in the trap. The broad asymmetric distribution is due to decays from neutral radioactive atoms occurring out of the trap and to accidental events.

The two main results are: i) that the signal to background ratio in the region of the peak is about 100:1 and ii) that the largest fraction of the background is confidently identified as being associated with decays occurring outside the trap, suggesting ways in which the setup can be improved for future precision measurements. This demonstrates that this system provides an efficient and clean preparation scheme for precision experiments at low energies.



## Conclusions and Future Prospects

Since the completion of the experiment presented above, the efficiency of the beam preparation system has been significantly improved. Furthermore, a new run has taken place at SPIRAL, with the aim of producing more than  $3 \times 10^6$  coincidences for a physics experiment. The goal has successfully been achieved, definitively establishing the proposed beam preparation and trapping scheme for trap assisted decay experiments.

## Acknowledgements

The LPCTrap facility described in this report is operated by a collaboration between LPC-Caen, GANIL and University of Huelva. The results presented above were obtained in the framework of the experiment E476S carried out at SPIRAL/GANIL.



# Development and validation of neutron detector simulations for EURISOL

Brian Roeder

LPC Caen

October 31, 2008 – v1.0

## Introduction

One set of experiments proposed for EURISOL seeks to investigate the character and structure of oxygen isotopes beyond the neutron drip line, namely  $^{25-28}\text{O}$ . Previously conducted experiments over the last 15 years have shown these nuclei to be unbound, even though the Fluorine isotopes with one more proton are bound until at least  $^{31}\text{F}$  ( $N=22$ ).

Modern shell model calculations from Brown et al. suggest that the even heavy oxygen isotopes,  $^{26,28}\text{O}$ , are only weakly unbound. Also, a recent measurement has shown  $^{25}\text{O}$  is unbound by  $\approx 770$  keV [1]. Therefore, unbound states in  $^{25-28}\text{O}$  should be accessible with “knockout” or “breakup” reactions from either the very neutron-rich Ne or F isotopes. Beams of these isotopes with reasonable intensities ( $> 104$  pps) should be available with the EURISOL facility.

For these experiments, it is necessary to detect neutrons over a wide range of energies ( $1 \text{ MeV} \leq E_n \leq 150 \text{ MeV}$ ), with high efficiency, and good energy and angular resolution. In addition, the experiments involving the detection of resonances from the decays of  $^{26-28}\text{O}$  require the ability to detect multiple neutrons and discriminate between neutron and  $\gamma$  ray events. To design a detector array optimized for these and other similar experiments, a Monte Carlo simulation with the package GEANT4 [2] has been developed. These simulations model 1) the distribution of the neutrons and charged recoil particles resulting from the breakup of the unbound nuclei and 2) the scattering of the neutrons inside the scintillation material. Using these simulations, realistic estimates of the efficiency and resolution for a given detector array geometry can be obtained.

It was found during this study that the neutron scattering models available in the GEANT4 package were not properly reproducing the measured detection efficiency of existing detectors. In addition, the angular distributions of the neutrons after scattering in the detector were found to be



incorrect, which resulted in inaccurate predictions of the detector cross-talk probability. For these reasons, the neutron scattering model MENATE\_R has been developed within the framework of GEANT4 to be used in place of the existing GEANT4 neutron scattering models.

Comparisons between MENATE\_R and the GEANT4 models are given in section 2. Section 3 gives a summary of the simulations that are planned with GEANT4 that will lead to a proposal for the design of the neutron detector array.

## Benchmarks for Neutron Scattering Models

The first step in developing a Monte-Carlo simulation for the neutron array was to include a reliable model for neutron scattering within scintillator materials. For the energy range concerned in this study ( $1 \text{ MeV} \leq E_n \leq 150 \text{ MeV}$ ), as well as its neutron -  $\gamma$  ray discrimination characteristics, the liquid scintillator BC-501A (formerly NE213) [3] was considered. Existing neutron detector arrays constructed using this material include DEMON [4], and EDEN [5] among others. In particular, detection efficiency measurements for DEMON modules have been conducted over a large range of energies [6], and measurements have been reported for the crosstalk probability between two modules as a function of detector threshold [4]. The ideal neutron scattering model used within a Monte-Carlo simulation would be able to accurately reproduce these experimental measurements to within a few percent.

In GEANT4, there is no “default” model for neutron scattering. However, within the GEANT4 framework, there exist several neutron scattering models that the user can choose. These models include purely data-based models such as the NeutronHP models, cross section parameterization-based models such as the LElastic and LENeutronInelastic models, and theory-based models such as the QElastic and G4PreCompound models. The models in GEANT4 all cover the range of energies needed for the neutron scattering except for the NeutronHP model. The NeutronHP model only includes neutron cross section data files up to 20 MeV, and thus does not cover the energy range needed for this study. The neutron scattering models can be chosen individually or in combination, usually with one specific model for the neutron elastic scattering and one specific model for the inelastic and reaction-type scattering. In addition, data sets of the total cross sections for the elastic or inelastic scattering of neutrons on a given nucleus can be included with the models to constrain the neutron interaction probability. Further details on the physics content of the neutron scattering models can be found on the GEANT4 webpage [7].

Simulations of the efficiency of a DEMON module [4] have been conducted assuming different GEANT4 included neutron scattering models. In these simulations, a DEMON module was approximated as a cylinder of BC-501A (NE213) scintillator 16cm in diameter by 20cm in length. The charged recoil particles resulting from the scattering of neutrons within the scintillator deposit energy in the detector according to the GEANT4 hMultipleScattering and ionIonisation models [2]. The total energy deposits in the detector for each event are then converted to light energy, or “electron-equivalent” (MeVee),



following the method of Ref. [8]. In all simulations, neutron- $\gamma$  ray discrimination is also taken into account by not including the light energy deposited in the detector from the  $\gamma$  ray scattering.

The results of the DEMON module efficiency simulations for a “pencil beam” (thin beam of neutrons along the z-axis of the module) and a “conic beam” (semi-isotropic beam of neutrons centered at 5m distance from the module and incident over the face of the module) are presented in figures 1 and 2. These results are compared with the experimental efficiency measurements for DEMON modules with Threshold = 500 MeVee [6]. The simulations that had the LElastic model included for the neutron elastic scattering over-predict the detection efficiency from 2-5 MeV, are near the data points from 5-20 MeV, and then consistently under-predict the efficiency from 20-150 MeV. The simulation with the LElastic and LENeutronInelastic models without the data set (green line) also includes a sudden drop in the efficiency between 32 and 33 MeV of 14% not present in the other models. This is believed to result from a discontinuity between the low energy and intermediate



### DEMON Efficiency Simulations (pencil beam)

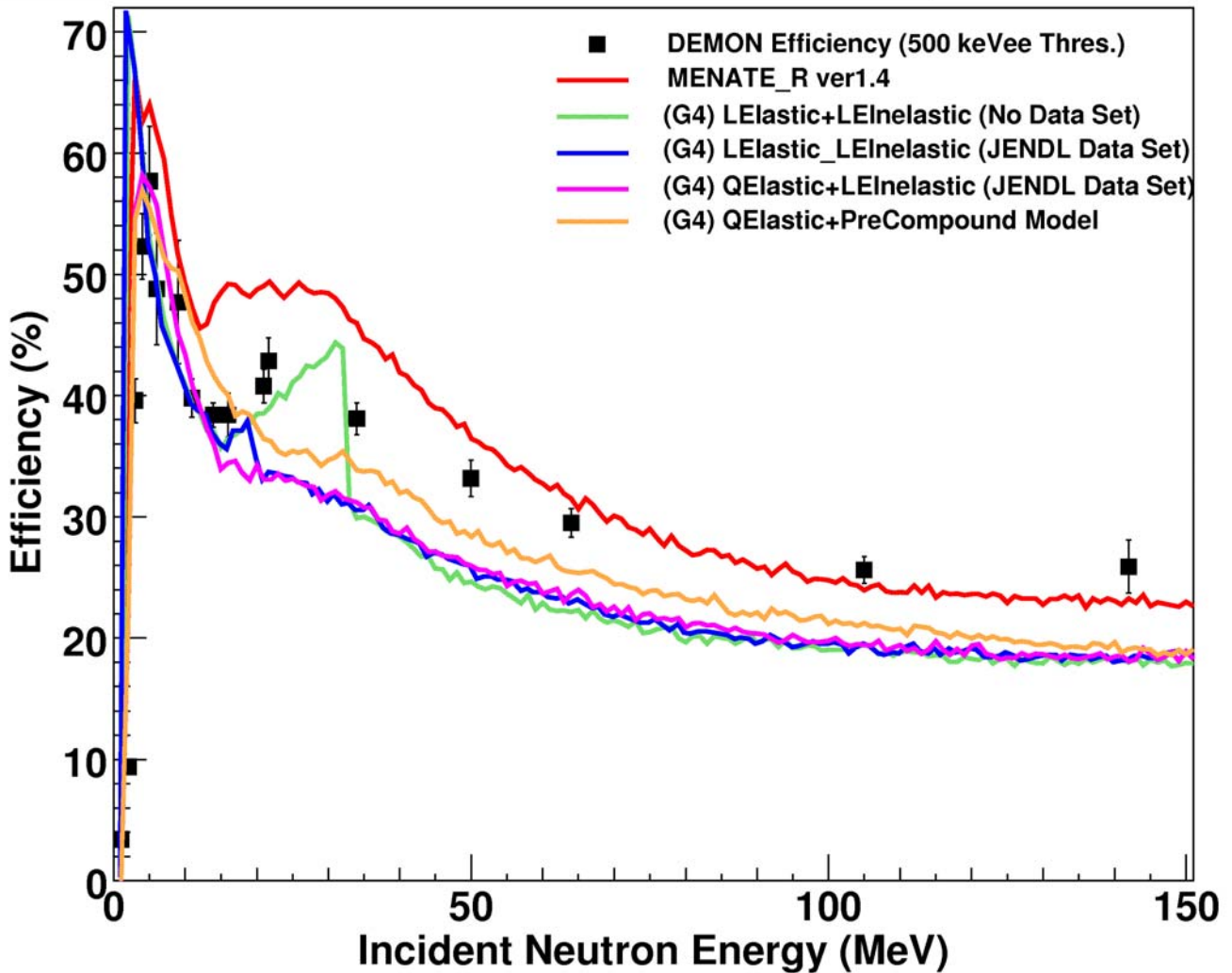


**Figure 1:** DEMON module efficiency simulations with pencil beam compared with measurements with a detector threshold of 500 keVee. See text for discussion.



**DEMON Efficiency Simulations (conic beam, 5m dist.)**

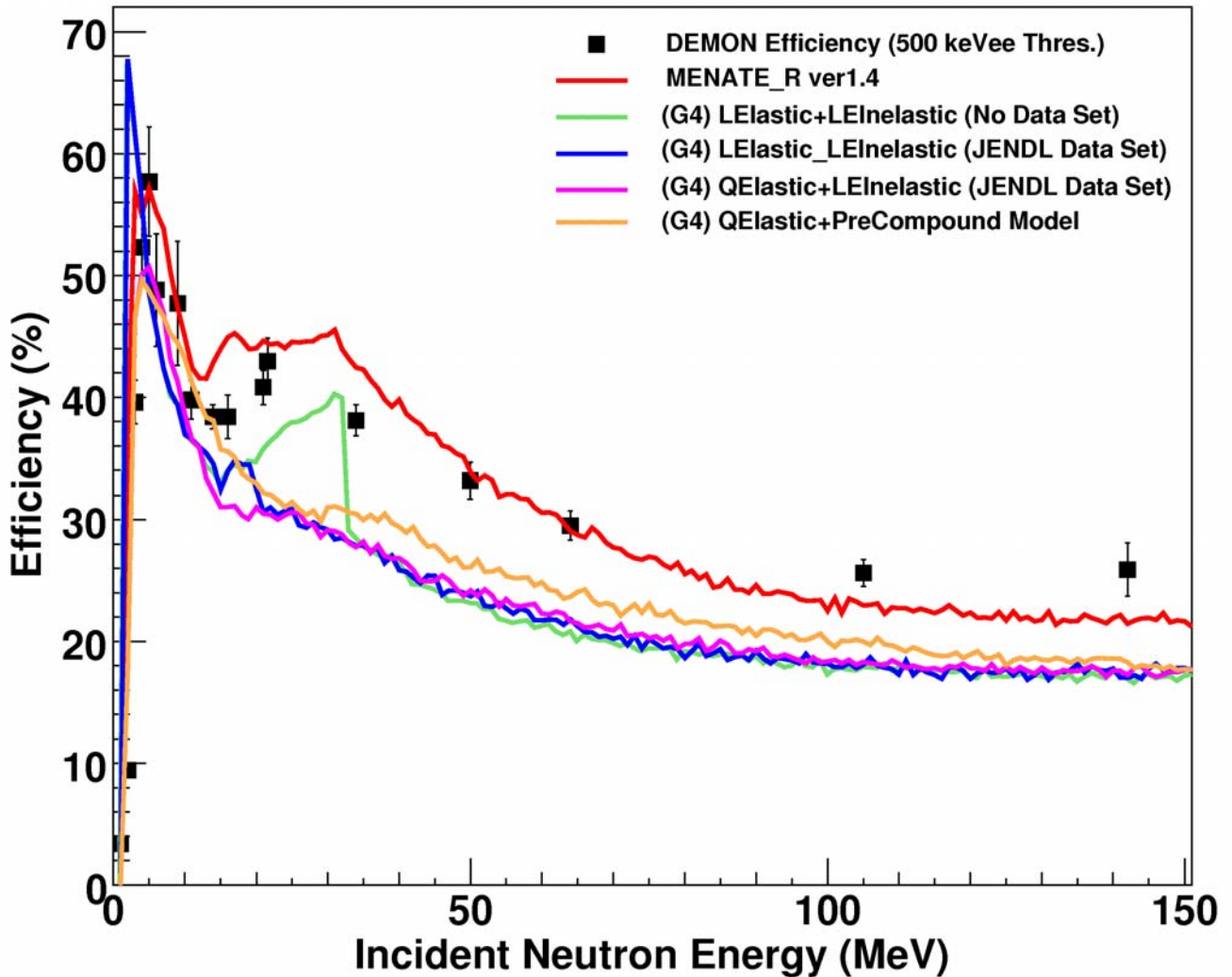


**Figure 2:** DEMON module efficiency simulations with a conic beam source 5m from the detector compared with measurements with a detector threshold of 500 keVee. The conic beam simulations better represent the manner in which the original experimental measurements were performed. See text for discussion.



energy cross section parameterizations in the LElastic model. Simulations with the theory-based Qelastic model give better results for the efficiency from 2-5 MeV, but also under-predict the efficiency for  $E_n > 25$  MeV. In addition, both inelastic scattering models have been noted to give unrealistic final states for the  $n+^{12}\text{C}$  reactions. For example, the inelastic scattering models do not include the  $^{12}\text{C}(n,n'+3\alpha)$  reaction properly, which is important for the DEMON module efficiency in the energy range 20 MeV-35 MeV as it contributes to an increase in the detection efficiency.

Previously, the efficiencies of DEMON and other detectors with liquid scintillator have been modelled with neutron scattering codes such as MENATE [9], the “Kent State” (KSU ) code [8], and DECOI [10]. All of these codes include total cross section data for  $n + p$  and  $n+^{12}\text{C}$  elastic and inelastic scattering as summarized by Ref. [11]. While the NeutronHP model in the GEANT4 toolkit takes a similar, data-based approach to modelling neutron scattering, it can not be used for neutrons with energies greater than 20 MeV and lacks cross sections for certain inelastic scattering reactions. Thus, in order to include features of the previously developed neutron scattering models within the GEANT4 framework and that are valid from  $1 \text{ MeV} \leq E_n \leq 150 \text{ MeV}$ , the model MENATE\_R has been developed. MENATE\_R is an updated version of the MENATE code [9] which includes an improved calculation of the neutron mean free path in liquid scintillator, improved models for the  $^{12}\text{C}(n,n'+3\alpha)$  and  $^{12}\text{C}(n,n'+\gamma)$  reactions, and parameterizations for the  $n + p$  and  $n+^{12}\text{C}$  elastic scattering angular distributions. The  $n + p$  and  $n+^{12}\text{C}$  elastic scattering cross sections were taken from the ENDF-VII compilation. The  $n+^{12}\text{C}$  inelastic total cross sections and the reactions considered are the same as in the previous codes [8, 11].

The efficiencies of a DEMON module as simulated with the MENATE\_R model used within the GEANT4 framework are shown by the red lines in figures 1 and 2. In the case of the “pencil beam”, the simulated efficiency follows the general trend of the data but over-predicts the detection efficiency up to about 65 MeV. The result is closer for the “conic beam” simulation, where the simulation follows most of the data points except for between 20-35 MeV and for  $E_n > 100$  MeV. The “conic beam” simulations better reproduce the experimental data points because they more closely resemble the manner in which the measurements were carried out. However, it has also been noted in previous work that the above codes, (including MENATE\_R), do not include the  $^{12}\text{C}(n,xd_0)$  reaction that contributes to the detection efficiency in the 20-35 MeV region [12]. Nevertheless, the current version of the MENATE\_R model gives a better description overall of the measured efficiency data for the DEMON module than the GEANT4 neutron scattering models.

Simulations were also carried out to model the cross-talk probability for two DEMON modules. Cross-talk is defined as when a single neutron is detected in multiple detector modules in the same event. Neglecting cross-talk results in an overestimation of detection efficiency for an array of detectors and artificial increases in multiple neutron events.

A measurement of the cross-talk for two DEMON modules was reported by Ref. [4]. In that measurement, two DEMON modules were placed 1.75m from a common source of neutrons and 20cm from each other.



apart. A beam of neutrons with  $E_n = 37$  MeV was directed at the first detector (M0) while the second detector (M1) was well shielded against the incident neutron beam. The total cross-talk probability for a given detection threshold was calculated in the experiment as  $Prob. = N_{01C}/N_{0S}$ ; the number of M0-M1 coincidences over the number of events detected in detector M0 for a given detection threshold in detector M1.

The results of simulation of the cross-talk probability measurement vs. detector threshold for module M1 are shown in figure 3. As in the efficiency simulations, the GEANT4 models are compared with the MENATE\_R model. The combination of the Qelastic and LENeutronInelastic models gives the best overall description of the data, and the combination of the LElastic and LENeutronInelastic models also gives results that are close to the measured values. However, these results are misleading because these same model combinations under-predict the DEMON detection efficiency at 37 MeV as shown in figures 1 and 2. If the efficiencies predicted by these model combinations were adjusted to fit the experimental data, their predictions for the cross-talk probability as compared with the data would increase.

The MENATE\_R model (red line) overestimates the cross-talk probability for low detection threshold in the second detector. However, once a detection threshold of 3 MeVee is reached in the second detector, the simulation reproduces the data within error. The overestimation of the cross-talk is caused by the overestimation in detection efficiency at 37 MeV predicted by MENATE\_R, and by the treatment of the angular distributions for  $n+^{12}\text{C}$  inelastic scattering within the model (the scattered neutron in the inelastic reactions is scattered isotropically).

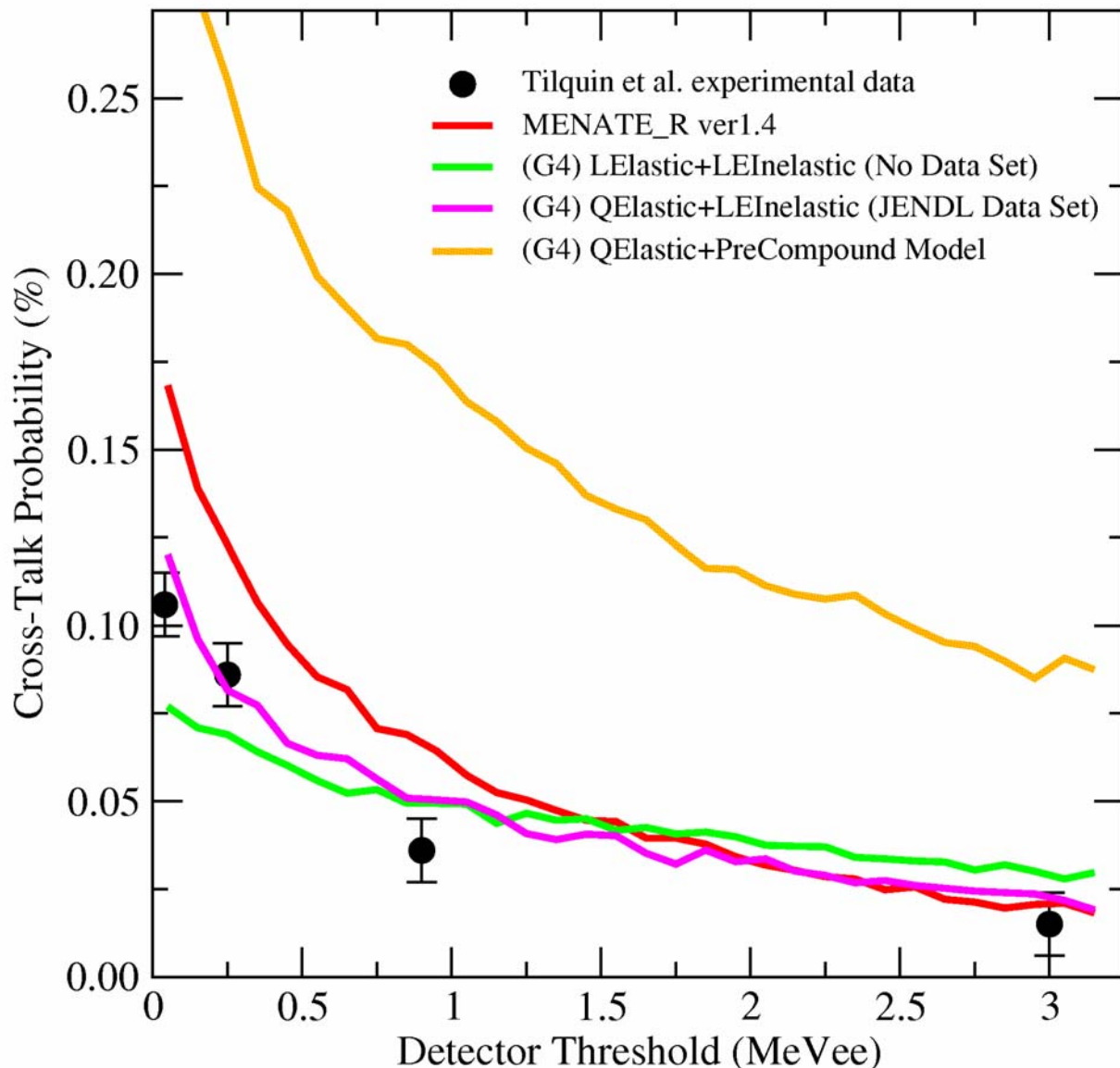


**Figure 3:** Detector cross-talk Probability vs. the Detector Threshold for the second detector as measured in Ref. [4] compared with different neutron scattering models in GEANT4. The agreement between the cross-talk data and the GEANT4 simulation with the QElastic+LEElastic models (pink line) is misleading because the detection efficiency in the simulations at 37 MeV is too low with this model combination (see figs. 1 and 2). The MENATE\_R model (red line) follows the general trend of the data and agrees with the data for high detection thresholds in detector M1. See text for further discussion.



in the centre of mass frame). Despite these problems, MENATE\_R can predict the general trend of the cross-talk probability in the data and correctly predicts the cross-talk if high detection thresholds are used. This makes the current version of MENATE\_R useful for modelling neutron detection at higher energies where 6 MeVee detection thresholds are typical.

In summary, the MENATE\_R model provides reasonable results for simulations of detection efficiency and cross-talk for detectors with BC-501A scintillator. As the model has been benchmarked for certain test cases, it can now be applied as the model used for neutron scattering in simulations of EURISOL neutron detector array designs.

## Conclusion and Future Prospects

The MENATE\_R neutron scattering model, when used within the GEANT4 framework, has demonstrated that it is possible reproduce measurements for neutron detection efficiency and detector cross-talk with Monte-Carlo simulations to within a few percent. With this model, various detector geometries can be investigated in order to determine which would best to use in breakup experiments for EURISOL. Some of the geometries currently being investigated include “modular-type” designs similar to DEMON [4] and “wall-type” designs similar to MONA [13] at NSCL/MSU and LAND [14] at GSI. A visualization of one of the preliminary “wall - type” geometries is shown in figure 4.

Improvements to the MENATE\_R model such as the addition of neutron scattering on inactive materials in the detectors and data for the differential cross sections for the  $n+^{12}\text{C}$  inelastic scattering reactions are desirable in order to increase its accuracy. The availability of total cross section and differential cross section angular distribution data over the energy range considered would allow the neutron scattering for these materials to be added to the model.

Nevertheless, investigations can be made with the current MENATE\_R model to determine neutron detector array designs that will allow for the detection of multiple neutron events while accounting for the effects neutron scattering in the detector and cross-talk. The results of the simulations of these various designs will be given in an upcoming report.

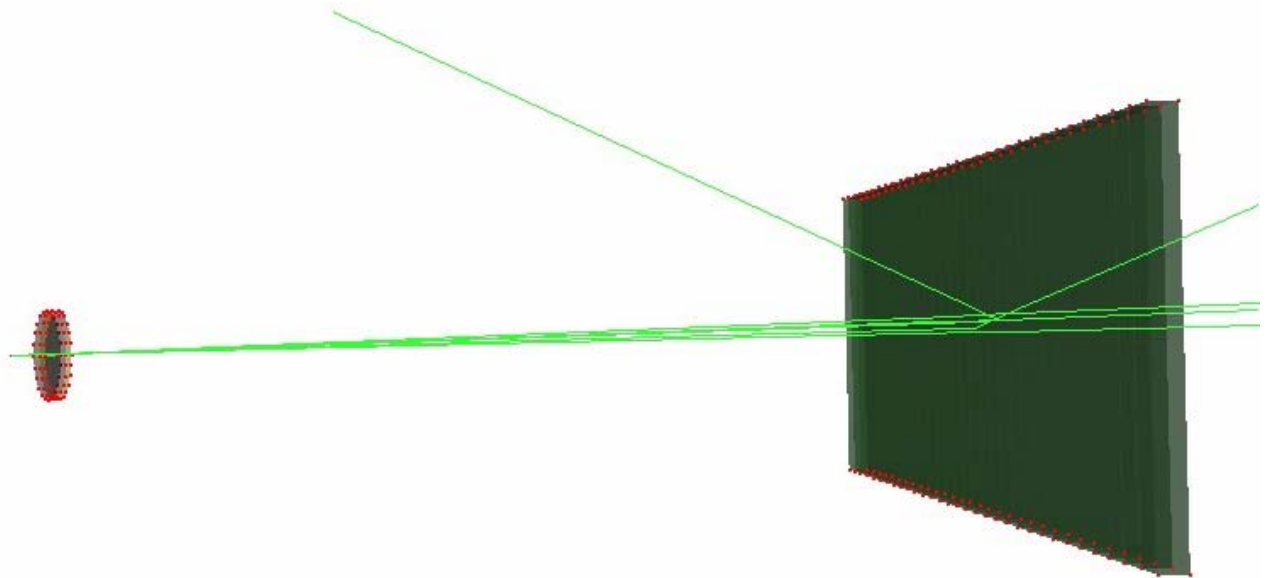


**Figure 4:** Visualization of the “Wall-type” neutron detector simulation in GEANT4. This represents one of the detector array designs being investigated.

### Acknowledgements

The author would like to acknowledge the contributions of M. Labiche for introductions to the use of the GEANT4 toolkit. Also acknowledged are F. M. Marques and J.L. Lecouey for helpful discussions.

### *REFERENCES*

- [1] C. R. Hoffman et al. Phys. Rev. Lett. 100, 152502 (2008).
- [2] S. Agostinelli et al. Nucl. Instr. and Meth. A506, pages 250–303, (2003). GEANT4 version 4.9.1.p02.



- [3] <http://www.detectors.saint-gobain.com>.
- [4] I. Tilquin et al. Nucl. Instr. and Meth. A365, pages 446–461, (1995).
- [5] H. Laurent et al. Nucl. Instr. and Meth. A326, pages 517–525, (1993).
- [6] C. Varignon. Ph.D. thesis - LPC Caen, (1999).
- [7] <http://geant4.cern.ch/support/userdocuments.shtml>.
- [8] R. A. Cecil, B. D. Anderson, and R. Madey. Nucl. Instr. and Meth. 161, pages 439–447, (1979).
- [9] P. D'ŷsesquelles et al. Nucl. Instr. and Meth. A307, pages 366–373, (1991).
- [10] J. F. Lecolley et al. - Private Communication.
- [11] A. Del Guerra. Nucl. Instr. and Meth. 135, page 337, (1976).
- [12] S. Meigo. Nucl. Instr. and Meth. A401, pages 365–378, (1997).
- [13] T. Baumann et al. Nucl. Instr. and Meth. A543, page 517, (2005).
- [14] Th. Blaich et al. Nucl. Instr. and Meth. A314, page 136, (1992).